Laser cooling of molecular internal degrees of freedom by a series of shaped pulses

Allon Bartana and Ronnie Kosloff
Department of Physical Chemistry and the Fritz Haber Research Center, the Hebrew University, Jerusalem 91904, Israel

David J. Tannor
Department of Chemistry and Biochemistry, University of Notre Dame, Notre Dame, Indiana 46556

(Received 4 January 1993; accepted 17 March 1993)

Laser cooling of the vibrational motion of a molecule is investigated. The scheme is demonstrated for cooling the vibrational motion on the ground electronic surface of HBr. The radiation drives the excess energy into the excited electronic surface serving as a heat sink. Thermodynamic analysis shows that this cooling mechanism is analogous to a synchronous heat pump where the radiation supplies the power required to extract the heat out of the system. In the demonstration the flow of energy and population from one surface to the other is analyzed and compared to the power consumption from the radiation field. The analysis of the flows shows that the phase of the radiation becomes the active control parameter which promotes the transfer of one quantity and stops the transfer of another. In the cooling process the transfer of energy is promoted simultaneously with the stopping population transfer. The cooling process is defined by the entropy reduction of the ensemble. An analysis based on the second law of thermodynamics shows that the entropy reduction on the ground surface is more than compensated for by the increase in the entropy in the excited surface. It is found that the rate of cooling reduces to zero when the state of the system approaches an energy eigenstate and is therefore a generalization of the third law of thermodynamics. The cooling process is modeled numerically for the HBr molecule by a direct solution of the Liouville von Neuman equation. The density operator is expanded using a Fourier basis. The propagation is done by a polynomial approximation of the evolution operator. A study of the influence of dissipation on the cooling process concludes that the loss of phase coherence between the ground and excited surface will stop the process.

I. INTRODUCTION

In cooling a molecular system, heat can be extracted either by an evaporative process or by a heat pump. Cooling means that a reduction of a system's entropy takes place, leading eventually to a completely ordered system at the absolute zero temperature. In an evaporative process this entropy reduction is more than compensated for by the entropy increase in evaporation. If a heat pump system is used on the other hand, the external work is used to drive a pump which disposes of the entropy in a heat sink.

The cooling of molecular ensembles is an important part of the experimental elucidation of molecular encounters. Entropy reduction is equivalent to a reduction of dispersion in molecular ensembles which will bring about a well defined initial state for the experiment. Cooling by seeded supersonic beams, for example, has revolutionized molecular spectroscopy of large molecules, as well as the study of van der Waals complexes.[1]

The development of monochromatic polarized laser light sources has created new possibilities for cooling processes. Since this ideal beam of light carries no entropy, in an evaporative process it can be anticipated that the beam is scattered, thus increasing its entropy while cooling the radiative coupled matter. This process is the basis of the Doppler laser cooling of the translational degrees of freedom demonstrated for sodium and other atoms.[2,3]

Radiative cooling of a molecular ensemble by an evaporative procedure can also be considered. Cooling is obtained by removing the excited vibrational population from the ground surface by transferring them to the excited surface, thus leaving a cooler ensemble downstairs. A possible procedure is to tune the laser light to one of the hot band transitions of the molecules. Then by adjusting the intensity and duration of the radiation, π pulse conditions can be obtained which will transfer all the population of the hot ground surface vibration to the excited surface. Such conditions can also be obtained by the adiabatic passage technique.[5]

The present study investigates a different cooling process driven by a synchronous heat pump which extracts power from the radiation. It is based on the thermodynamic pure work property of coherent light. The setup is designed to cool molecules on their ground electronic surface with the excess entropy dissipated on to the excited surface. The system to be cooled consists of the vibrational manifold of the ground electronic surface of a molecule. This surface is radiatively coupled to the excited electronic surface which serves as the heat sink. The phase of the radiation is controlled, maintaining a constant population on the ground surface. The cooling process of an ensemble of molecules reduces the vibrational dispersion of the molecules residing on the ground electronic surface. At the

 0021-9606/93/99(1)/196/15/$6.00

same time, the molecules residing on the excited electronic surface become vibrationally hot.

The processes of cooling an ensemble of molecules with laser beams are first demonstrated on an ideal ensemble of noninteracting molecules. Ultimately, however, a more realistic approach must consider the possibility of interactions between the molecules. Such interaction which leads to dissipation is analyzed in this work in relation to its influence on the performance of the heat pump.

The cooling method developed in the present study is an offspring of research devoted to active control of molecular processes.[4–12] Again, one can identify two basic approaches applied to chemical control. The first is an adiabatic approach where the control mechanisms are applied on a time scale which is slow in relation to the molecular motion.[5,6] The evaporative process is of this class since it is based on the ability to tune frequency, amplitude and duration of a laser pulse to be slow or adiabatic on the time scale of vibrational motion but fast on the time scale of molecular collisions. The other approach is an impulsive intervention which is fast on the molecular time scale.[7–9] In the heat pump method the cooling is impulsive and can be made faster than the competing parasitic heating processes. A general formulation of the control of chemical encounters has been dealt with in the theory of optimal control.[7,10]

The present study is a development of a method[12] originally intended to excite the ground surface vibration of a molecule impulsively while minimizing radiative damage.[13] A description of cooling requires a statistical ensemble approach, and therefore, the previous study, which was formulated in a wave function description cannot address the problem. In the present research, the process is formulated within a Liouville space description[14] allowing a full statistical approach including the calculation of entropy and temperature. This description is used to draw analogs to the laws of thermodynamics.

Abstract thermodynamics consists of objects or systems with membranelike partitions separating them. The transport properties of the membranes define the interaction between the systems. The membranes are permeable to certain quantities and nonpermeable to others. For example, a membrane can allow transport of heat but be impermeable to mass transport of a specific chemical substance. Biological membranes have an additional quality of being selective in that they can actively promote the transport of a specific quantity at the expense of energy. In the heat pump model under investigation an analogy is drawn between this type of active transport and a quantum mechanical model of two subsystems which are radiatively coupled. The correspondence between quantum mechanics and thermodynamics is followed, by investigating the quantum versions of the three laws of thermodynamics. The dynamical model developed in this section allows the study of the interplay between the motion generated by the internal Hamiltonian, the radiative coupling, and the dissipation.

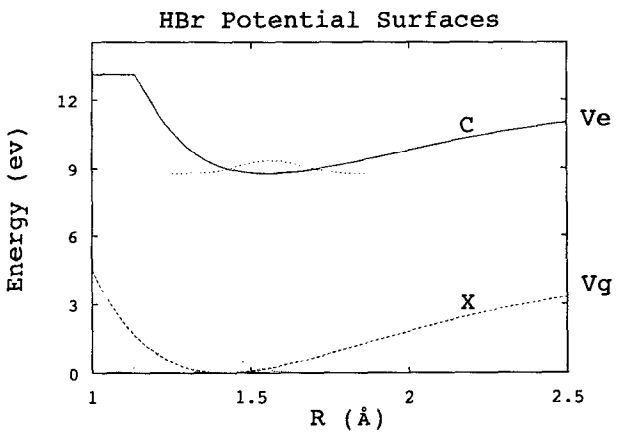

FIG. 1. Ground ($X\,^1\Sigma^+$) and the ($C\,^1\Pi$) excited potential energy surfaces of HBr.

II. THE RADIATIVE QUANTUM MECHANICAL MODEL

The basic model consists of an ensemble of identical molecules classified according to their possession of a quantity. For example, the quantity can be defined by the number of molecules with position to the right or to the left of a membrane. Quantum mechanically such a quantity is represented by a projection operator $\hat{\mathbf{P}}_\mathbf{g}$ and its inverse $\hat{\mathbf{Q}}_\mathbf{e}=\hat{\mathbf{I}}-\hat{\mathbf{P}}_\mathbf{g}$ so that $\hat{\mathbf{P}}_\mathbf{g}+\hat{\mathbf{Q}}_\mathbf{e}=\hat{\mathbf{I}}$. The specific form of the projection operator, used in this study, is realized by considering two distinct electronic surfaces. The molecules either reside on the ground electronic surface or on the excited electronic surface. As an explicit example the electronic potential surfaces of the HBr molecule are shown in Fig. 1. The internal state of the molecule is defined by the density operators $\rho_\mathbf{l}$, $\mathbf{l}\in\mathbf{g}$, $\mathbf{e}$ which are the indexes of the ground and excited surfaces, respectively.[14] The combined density operator describing the state of the combined ensemble can be written as

$$\hat{\rho}=\hat{\rho}_\mathbf{g}\otimes\hat{\mathbf{P}}_\mathbf{g}+\hat{\rho}_\mathbf{e}\otimes\hat{\mathbf{P}}_\mathbf{e}+\hat{\rho}_\mathbf{i}\otimes\hat{\mathbf{S}}_+ +\hat{\rho}_\mathbf{i}^\dagger\otimes\hat{\mathbf{S}}_- \tag{2.1}$$

where the tensor product of the internal space and the surface designation is used. Where $\hat{\mathbf{P}}_\mathbf{l}$ are projection operators on the surface, $\mathbf{l}$ and $\hat{\mathbf{S}}_\pm$ are the raising and lowering operators from one surface to the other. The algebraic relations of the operators $\hat{\mathbf{P}}_\mathbf{l}$ and $\hat{\mathbf{S}}_\pm$ can be calculated from the equivalent relations of the 2×2 Pauli matrixes. This combined state function takes into consideration the nonlocal character of quantum mechanics by introducing nondiagonal correlations between the ground and excited surfaces represented by the operator $\hat{\rho}_\mathbf{i}$.

The Hamiltonian of the system consists of the sum of internal Hamiltonians and an interaction term

$$\hat{\mathbf{H}}=\hat{\mathbf{H}}_0+\hat{\mathbf{V}}_t, \tag{2.2}$$

where the zero order Hamiltonian is the sum of the two separate parts,

$$\hat{\mathbf{H}}_0=\hat{\mathbf{H}}_\mathbf{g}\otimes\hat{\mathbf{P}}_\mathbf{g}+\hat{\mathbf{H}}_\mathbf{e}\otimes\hat{\mathbf{P}}_\mathbf{e} \tag{2.3}$$

and the surface Hamiltonians $\hat{\mathbf{H}}_\mathbf{l}$ are functions of internal coordinates. The interaction part controls the transport

properties of the membrane separating the systems. In this study, it contains only radiatively coupling terms

$$\hat{V}_t = -\hat{\mu} \otimes (\hat{S}_+ \epsilon + \hat{S}_- \epsilon^*) \tag{2.4}$$

where $\hat{\mu}$ is the transition dipole operator and $\epsilon(t)$ represents a semiclassical time dependent radiation field.

The evolution is described by the Liouville von Neumann equation[14]

$$\frac{\partial \hat{\rho}}{\partial t} = -\frac{i}{\hbar}[\hat{H},\hat{\rho}] + \mathcal{L}_D(\hat{\rho}) \tag{2.5}$$

where the first term represents dynamics generated by the Hamiltonian, and the second term represents the dynamics generated by the dissipation. This equation represents the dynamics of an open quantum mechanical system under the restriction of a dynamical semigroup evolution.[15-18] Alternatively to Eq. (2.5), one can use the Heisenberg equations of motion to calculate the change in time of an explicitly time dependent operator

$$\frac{d\hat{A}}{dt} = \frac{\partial \hat{A}}{\partial t} + \frac{i}{\hbar}[\hat{H},\hat{A}] + \mathcal{L}_D^*(\hat{A}), \tag{2.6}$$

where the first term represents the explicit time dependence of the operator, the second term the Hamiltonian evolution, and the third term the dissipation which is the Hiesenberg version of the dissipative superoperator in Eq. (2.5).

III. THE TRANSPORT EQUATIONS AND THE FIRST LAW

Thermodynamic insight can be gained by studying the total change in energy representing the first law of Thermodynamics. Additional insight is gained by considering the population and energy currents from one system to the other. These currents flowing through the membrane, represent the balance equations. Within the model of Sec. II, the total energy change becomes

$$\frac{d\langle E\rangle}{dt} = \left\langle \frac{\partial \hat{H}}{\partial t} \right\rangle + \langle \mathcal{L}_D^*(\hat{H})\rangle, \tag{3.1}$$

where the second term of Eq. (2.6) is zero, since the Hamiltonian commutes with itself. This equation can be interpreted as the time derivative of the first law of thermodynamics[19,20] with the identification of power as

$$P = \left\langle \frac{\partial \hat{H}}{\partial t} \right\rangle \tag{3.2}$$

which is the time derivative of the work. The heat flow is

$$\dot{Q} = \langle \mathcal{L}_D^*(\hat{H})\rangle. \tag{3.3}$$

With these definitions, the power absorbed from the field into the system in the model of Sec. II becomes:

$$P = -\langle \hat{\mu} \otimes (\hat{S}_+ \dot{\epsilon} + \hat{S}_- \dot{\epsilon}^*)\rangle = -2\,\mathrm{Real}(\langle \hat{\mu} \otimes \hat{S}_+\rangle \cdot \dot{\epsilon}). \tag{3.4}$$

The term $\langle \hat{\mu} \otimes \hat{S}_+\rangle$ will reappear in many of the derivations and will be called the instantaneous dipole expectation.

Considering the population balance conditions, the total population is conserved, therefore

$$dN_g + dN_e = 0. \tag{3.5}$$

The flow of population across the membrane from one electronic surface to the other can be calculated using Eq. (2.6)

$$\frac{dN_g}{dt} = \frac{d\langle \hat{P}_g\rangle}{dt} = \frac{i}{\hbar}\langle [\hat{V}_t,\hat{P}_g]\rangle + \langle \mathcal{L}_D^*(\hat{P}_g)\rangle. \tag{3.6}$$

If dissipative nonradiative couplings between the ground and excited surfaces are not important, i.e., $\mathcal{L}_D^*(\hat{P}_g) = 0$, the ground surface population change for the model of Sec. II becomes

$$\frac{dN_g}{dt} = -\frac{i}{\hbar}\langle \hat{\mu} \otimes (\hat{S}_+ \epsilon - \hat{S}_- \epsilon^*)\rangle = \frac{2}{\hbar}\,\mathrm{Imag}(\langle \hat{\mu} \otimes \hat{S}_+\rangle \epsilon). \tag{3.7}$$

The flow of energy from the ground state can be calculated under the assumptions of small electronic dephasing, i.e., $\mathcal{L}_D^*(\hat{P}_g) = 0$ and also pure vibrational dephasing, i.e., $\mathcal{L}_D^*(\hat{H}_g) = 0$. Physically these conditions apply when the rate of relaxation to equilibrium is slow compared to the loss of phase ($T_2 \gg T_1$). Under these conditions

$$\frac{dE_g}{dt} = \frac{2}{\hbar}\,\mathrm{Imag}(\langle \hat{\mu}\hat{H}_g \otimes \hat{S}_+\rangle \epsilon). \tag{3.8}$$

When the total energy balance is considered, the power uptake can be distributed into the "bulk" of ground and excited surfaces as well as into a membrane entity which is equivalent to energy stored by the interaction. Since the interaction term is proportional to the field ϵ, for a pulsed field for which $\epsilon = 0$ at $t = \pm\infty$, one can consider the energy flow into the bulk by integrating Eq. (3.4) by parts, obtaining

$$\int_{-\infty}^{\infty} P\,dt = \int_{-\infty}^{\infty} \frac{\partial \langle \hat{\mu}\rangle}{\partial t}\,\epsilon\,dt = \int_{-\infty}^{\infty} \frac{dE_g}{dt}\,dt + \int_{-\infty}^{\infty} \frac{dE_e}{dt}\,dt. \tag{3.9}$$

This equation can be interpreted as the energy balance equation. The boundary term $-2\,\mathrm{Real}[\langle \hat{\mu} \otimes \hat{S}_+\rangle \epsilon(t)]$ which goes to zero when deriving Eq. (3.9), represents the transient loading of the system. In the thermodynamic framework the transient loading term is a surface term representing energy stored in the membrane. If the surface term becomes small in comparison to the volume terms E_g and E_e then one can omit the integral in Eq. (3.9) and obtain

$$dE = dE_g + dE_e. \tag{3.10}$$

Equation (3.10) can also be obtained within the limit of weak fields. Such balance equations represent one of the main tools of thermodynamic investigation. A schematic view of the thermodynamic currents can be seen in Fig. 2.

The spatial derivative of the loading term represents the internal force which the electromagnetic field exerts on the molecule

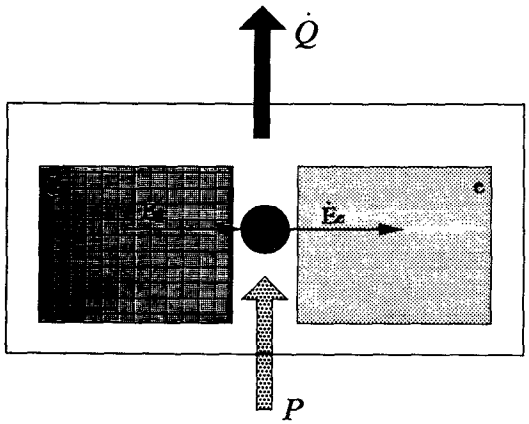

FIG. 2. Schematic diagram of the thermodynamic flows in the radiative quantum mechanical model.

$$\mathbf{F}=-2\,\mathrm{Real}(\langle\nabla_r\hat{\mu}\otimes\hat{\mathbf{S}}_+\rangle\epsilon) \tag{3.11}$$

where ∇_r is the gradient with respect to the internal coordinates. Combined with the conditions imposed in the next section in Eq. (4.8); one can apply a directional force on the molecule. The study of these possibilities will be described in future work.

Equations (3.4), (3.7), and (3.8) constitute the transport equations from one surface to the other. The next section, describes the control of the transport by manipulating the phase of the transient field ϵ.

IV. CONTROL OF TRANSPORT

The cooling process, as well as other molecular transport processes can be promoted either by controlling the field ϵ or its time derivative $\dot{\epsilon}$. This possibility stems from the fact that the transport equations Eq. (3.7) and Eq. (3.8) have a similar structure consisting of the real part of a product of a molecular expectation value $\langle\hat{\mathbf{X}}\rangle$ by the field ϵ. A similar structure is found in Eq. (3.4) where the transport is controlled by the real part of the product of a molecular expectation and the time derivative of the field. This structure can be expressed for Eq. (3.7) as

$$\frac{dN_g}{dt}=\frac{2}{\hbar}|\langle\hat{\mu}\otimes\hat{\mathbf{S}}_+\rangle||\epsilon|\sin(\phi_\mu+\phi_\epsilon), \tag{4.1}$$

where ϕ_μ is the phase angle of the instantaneous dipole and ϕ_ϵ is the phase angle of the radiation field. The physical interpretation of this angle is the sum of the angle of the induced polarization of the molecule and the angle of the polarization of the light. In a similar way

$$P=-2|\langle\hat{\mu}\otimes\hat{\mathbf{S}}_+\rangle||\dot{\epsilon}|\cos(\phi_\mu+\phi_{\dot{\epsilon}}) \tag{4.2}$$

and

$$\frac{dE_g}{dt}=\frac{2}{\hbar}|\langle\hat{\mu}\hat{\mathbf{H}}_g\otimes\hat{\mathbf{S}}_+\rangle||\epsilon|\sin(\phi_{\mu\mathrm{H}}+\phi_\epsilon), \tag{4.3}$$

where $\phi_{\mu\mathrm{H}}$ is the phase angle of $\langle\hat{\mu}\hat{\mathbf{H}}_g\otimes\hat{\mathbf{S}}_+\rangle$. From this description, it is clear that the control parameter of the transport quantities is the phase angle $\phi=\phi_i+\phi_j$. The most simple example is a monochromatic circularly polarized pulse for which $\epsilon(t)=Ae^{-i\omega t}$, where A is a slowly varying envelope function. For this pulse the phase angle of $\dot{\epsilon}$ is 90° rotated from the direction of ϵ, $\phi_{\dot{\epsilon}}=\phi_\epsilon-\pi/2$. Examining Eqs. (4.1) and (4.2) one obtains the relation

$$P=-\hbar\omega\frac{dN_g}{dt}. \tag{4.4}$$

This means that the system behaves as an effective two-level system where the power absorbed is linearly proportional to the population transfer.

For more general pulse shapes, using the above analysis, the control of the transport can be classified as being active or passive. For active control conditions the angle is

$$\phi_\mu+\phi_{\dot{\epsilon}}=\begin{cases}0\\ \pi\end{cases}\Rightarrow\begin{matrix}\text{maximum energy absorption}\\ \text{maximum energy emission}\end{matrix}, \tag{4.5}$$

$$\phi_\mu+\phi_\epsilon=\begin{cases}\frac{1}{2}\pi\\ -\frac{1}{2}\pi\end{cases}\Rightarrow\begin{matrix}\text{maximum positive mass transport}\\ \text{maximum negative mass transport}\end{matrix}, \tag{4.6}$$

$$\phi_{\mu\mathrm{H}}+\phi_\epsilon=\begin{cases}\frac{1}{2}\pi\\ -\frac{1}{2}\pi\end{cases}\Rightarrow\begin{matrix}\text{maximum energy intake to ground surface}\\ \text{maximum energy disposal from ground surface.}\end{matrix} \tag{4.7}$$

Even more important are passive controls where the transport of a certain quantity is blocked. If the phase angle is

$$\phi_\mu+\phi_{\dot{\epsilon}}=\pm\tfrac{1}{2}\pi\Rightarrow\text{zero total energy change,} \tag{4.8}$$

$$\phi_\mu+\phi_\epsilon=0,\pi\Rightarrow\text{zero mass transport,} \tag{4.9}$$

$$\phi_{\mu\mathrm{H}}+\phi_\epsilon=0,\pi\Rightarrow\text{zero change in ground surface energy.} \tag{4.10}$$

On examining the passive control conditions in Eqs. (4.8), (4.9), and (4.10) it can be noticed that there are two values of $\phi_i+\phi_j$ for which zero transport conditions apply. This fact can be utilized to simultaneously block the transport of one quantity and to select the direction of the transport of another quantity. A note of caution is needed at this point because naively it would seem that there is a meaning to the absolute phase of the field and to the phase of the molecular expectation values. But as will be seen in Sec. V, all phases have to be related to a previous synchronization pulse which synchronized the molecular clock with the field clock.

Figure 3 shows the phase angle conditions leading to different transport quantities. Figure 3(a) shows the phase angles for which the total power absorption is zero. Since no energy is absorbed or emitted from the field these conditions define laser catalysis.[21] Figure 2(b) shows the phase angle relations leading to zero mass transport. Figure 3(c) is of a RWA pulse corresponding to Eq. (4.4), where the mass transport is directed from the ground to the excited surface. Figure 3(d) shows the phase conditions which stop mass transport while monotonically di-

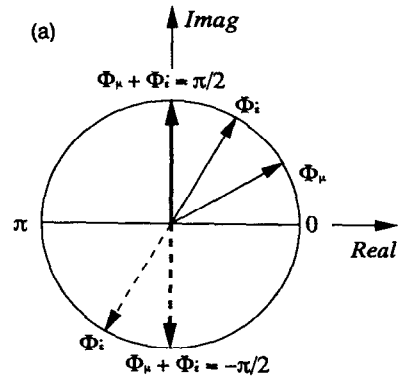

Zero Power Output

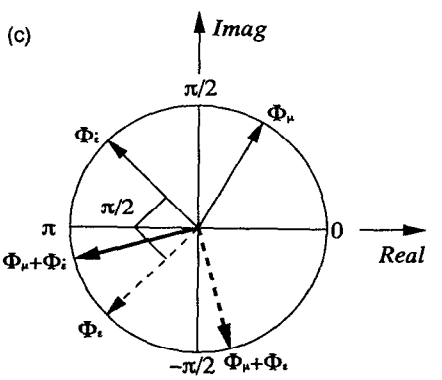

RWA Pulse

$\mathrm{Cos}(\Phi_\mu + \Phi_\epsilon) = \mathrm{Sin}(\Phi_\mu + \Phi_\epsilon)$

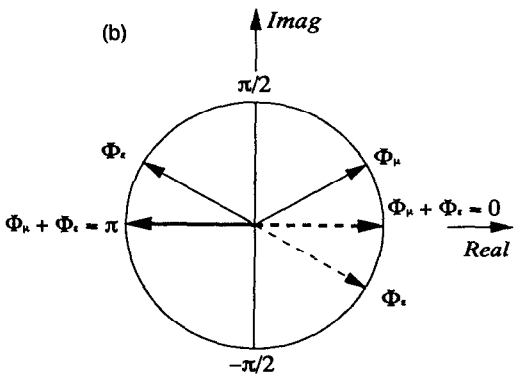

Zero Mass Transport

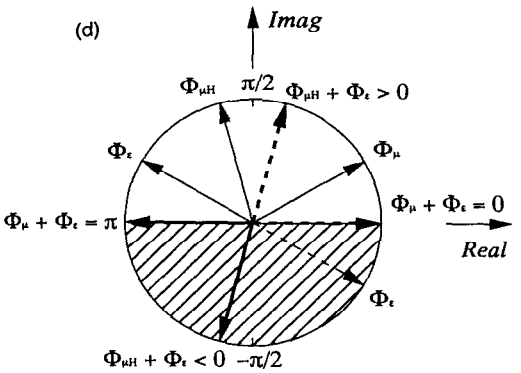

Zero Mass Transport With Monotonic Decrease in Ground Surface Energy

FIG. 3. (a) Phase angle diagram for zero power output. (b) Phase angle diagram for zero mass transport. (c) Phase angle diagram for a RWA pulse. (d) Phase angle diagram for zero mass transport and for a monotonic decrease in energy. The shaded area represents the region of phase angle of energy decrease in the ground surface.

recting energy out of the ground surface. These are the conditions of laser cooling studied in the next section.

V. LASER COOLING WITH ZERO MASS TRANSPORT

An active partition which is opaque to population transfer is obtained when the radiation field has the form

$$\epsilon = C(t)\Phi(\langle \hat{\mu} \otimes \hat{\mathbf{S}}_- \rangle), \tag{5.1}$$

where $C(t)$ is a real function of time and $\Phi(X) = X/|X| = e^{i\phi}$ is the phase factor. Equation (5.1) is another formulation of the conditions in Eq. (4.9). Active control requires the expectation value of the instantaneous dipole $\langle \hat{\mu} \otimes \hat{\mathbf{S}}_+ \rangle$ to be nonzero. Starting when all the population is on the ground surface will lead to a zero value instantaneous dipole. The procedure adopted in this study in order to create a nonzero term, is to apply a strong short pulse which transfers a small amount of population to the excited surface accompanied by a nonzero instantaneous dipole. This process serves to synchronize the molecular motion and the radiative field. Once these conditions are established the control process can proceed. Under the conditions of Eq. (5.1) the total change in energy has two components one of which is

$$P_1 = -2\dot{C}(t)\,|\langle \hat{\mu} \otimes \hat{\mathbf{S}}_+ \rangle| \tag{5.2}$$

the power associated with loading the system. The second component is

$$P_2 = \frac{2}{\hbar} C(t)\,\mathrm{Imag}[\Phi(\langle \hat{\mu} \otimes \mathbf{S}_+ \rangle)\langle (\hat{\mathbf{H}}_g \hat{\mu} - \hat{\mu}\hat{\mathbf{H}}_e) \otimes \hat{\mathbf{S}}_- \rangle], \tag{5.3}$$

which is the power required to drive the heat pump. Under the conditions of zero mass transport, the change of the energy on the ground state becomes

$$\frac{d\langle E_g \rangle}{dt} = C(t)\frac{2}{\hbar}\,\mathrm{Imag}[\Phi(\langle \hat{\mu} \otimes \hat{\mathbf{S}}_- \rangle)\langle \hat{\mu}\hat{\mathbf{H}}_g \otimes \hat{\mathbf{S}}_+ \rangle]. \tag{5.4}$$

The condition on the function $C(t)$ that will lead to a monotonic decrease in energy becomes

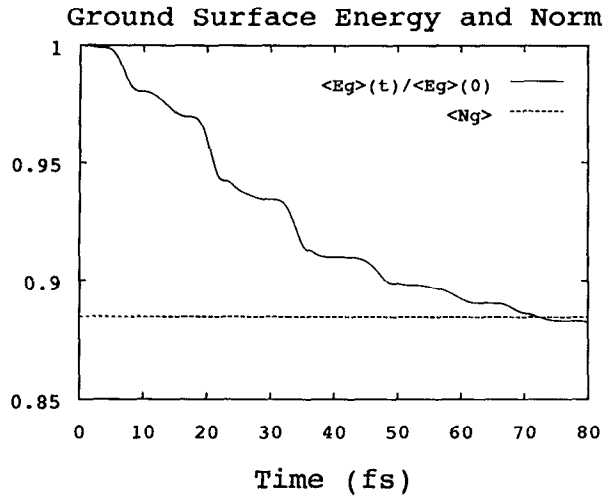

FIG. 4. The ground surface energy $\bar{E}_g$ and norm $\langle \hat{\mathbf{P}}_g \rangle$ as a function of time for a pulse shape shown in Fig. 9, for the HBr molecule. The potential energy surfaces are shown in Fig. 1. The energy is normalized to its initial value.

$$C(t) \propto -\frac{2}{\hbar} \mathrm{Imag}[\Phi(\langle \hat{\mu} \otimes \hat{\mathbf{S}}_- \rangle)\langle \hat{\mu}\hat{\mathbf{H}}_g \otimes \hat{\mathbf{S}}_+ \rangle]. \quad (5.5)$$

In Fig. 4, a monotonic decrease in energy is observed as a result of a pulse shape calculated according to Eq. (5.5). The resulting pulse shape is shown in Figs. 9, 10, and 11. In Sec. VI it will be shown that the energy decrease in the ground surface is accompanied by an entropy reduction (Fig. 7) which therefore meets the thermodynamic criteria of cooling.

The strategy of cooling using the pulse shape of Eq. (5.5), is only one of many possibilities. Therefore, it can be asked what is the optimal strategy for minimizing the ground surface energy with minimum power consumption under the restriction of zero mass transport? An optimization solution local in time to the question can be obtained by minimizing the functional

$$J = \frac{d\langle \hat{\mathbf{H}}_g \otimes \hat{\mathbf{P}}_g \rangle}{dt} + W|\epsilon|^2, \quad (5.6)$$

where W is a penalty function imposed by the power consumption. The variation of J, δJ is with respect to $\delta C(t)$, since the phase is restricted by the zero population transfer condition Eq. (5.1). Carrying out the calculation leads to Eq. (5.5) with the proportionality constant equal to $1/2W$. This local solution can be replaced with a global one, minimizing the ground surface energy $J=E_g$ at a specific final time t_f with the minimal cost of external pumping energy $\int_0^{t_f} P\,dt$.

The objective is to minimize the ground surface energy $E_g(t_f)$.

The constraints are

(a) evolution governed by the Liouville von Neumann equation $\partial\hat{\rho}/\partial t = \mathcal{L}(\hat{\rho})$;

(b) zero mass transport $dN_g = 0$;

(c) restricted total power consumption $\bar{E} = \int_0^{t_f} |\epsilon|^2\,dt$.

The initial state of the system is set as $\hat{\rho}(0)$. By defining the Lagrange multipliers, the objective functional can be minimized subject to the constraints. This leads to the modified objective functional $\bar{J}$

$$\bar{J} = \mathrm{tr}[\hat{\mathbf{H}}_g \otimes \hat{\mathbf{P}}_g \hat{\rho}(t_f)] + \int_0^{t_f} \mathrm{tr}\left\{\left[\frac{\partial\hat{\rho}}{\partial t} - \mathcal{L}(\hat{\rho})\right]\hat{\mathbf{B}} + \lambda|\epsilon|^2\right\} dt, \quad (5.7)$$

where $\hat{\mathbf{B}}$ is an operator Lagrange multiplier and λ is a scalar Lagrange multiplier. The variation of $\bar{J}$ is with respect to $\delta\hat{\rho}$ and $\delta|\epsilon|$. The condition $(dN_g/dt)=0$ determines the phase of ϵ through Eq. (4.9) or Eq. (5.1). It therefore is omitted from the variation. Calculating the variation of Eq. (5.7) and integrating by parts leads to the following equations:

(a) A forward equation for the density operator $\hat{\rho}$

$$\frac{\partial\hat{\rho}}{\partial t} = \mathcal{L}(\hat{\rho}) \quad (5.8)$$

subject to the initial condition $\hat{\rho}(0)$.

(b) A backward equation for the Lagrange operator $\hat{\mathbf{B}}$,

$$-\frac{\partial\hat{\mathbf{B}}}{\partial t} = \mathcal{L}^*(\hat{\mathbf{B}}) \quad (5.9)$$

subject to the final condition $\hat{\mathbf{B}}(t_f) = \hat{\mathbf{H}}_g \otimes \hat{\mathbf{P}}_g$. The dissipative part of Eq. (5.9) is symmetric in time, meaning that dissipation takes place in the forward as well as backward evolution.

(c) and the condition on the field

$$|\epsilon(t)| = \frac{1}{2\lambda}\mathrm{tr}\left\{\frac{\partial\mathcal{L}[\hat{\rho}(t)]}{\partial|\epsilon|}\hat{\mathbf{B}}(t)\right\} = -\frac{1}{2\lambda}\left\langle\frac{\partial\mathcal{L}^*[\hat{\mathbf{B}}(t)]}{\partial|\epsilon|}\right\rangle. \quad (5.10)$$

Equation (5.10) can be interpreted as the scalar product of a forward moving density, and of a backward moving time-dependent operator. The optimal field at time t is determined by a time-dependent objective function propagated from the target time t_f backwards to time t. An image of the optimal process is of shooting a moving target. A similar equation for optimal chemical control in Liouville space has been derived by a different method by Yan *et al.*[22]

In dissipative dynamics, the backwards propagating target operator decays into a stationary operator and therefore, its change in time becomes zero $\mathcal{L}^*[B(-\infty)]=0$. This leads to loss of control, as can be seen in Eq. (5.10).

In the cooling process, the target operator is the ground surface operator $\hat{\mathbf{H}}_g(t_f)$. In general for weak field excitation, the target operator $\hat{\mathbf{B}}(t)$ can be expanded in powers of the field ϵ^k. For the cooling scheme under these conditions the target function becomes time independent and is just the Schrödinger picture operator $\hat{\mathbf{H}}_g$. Inserting the target function into Eq. (5.10) one obtains the result of Eq. (5.5) with the proportionality constant becoming $1/2\lambda$. As a conclusion the phase and amplitude conditions for cooling suggested in Eq. (5.5) are the optimal control

solutions for weak fields. They can be used also as a first guess for the optimal field in an iterative solution for strong fields.[23]

VI. THE SECOND LAW

Einstein, in a discussion in 1914,[24] realized that a quantum system which possesses a measurable quantity ϵ_i from a discrete spectrum, can be considered a separate chemical entity. This means that the mixing entropy associated with the dispersion of this quantity becomes

$$S(\bar{A}) = -k_B \sum_i P_i \log P_i, \tag{6.1}$$

where k_B is the Boltzman constant ($k_B=1$ in the rest of this paper) and $P_i=\langle \hat{\mathbf{P}}_i \rangle$ is the expectation value of the ith projection operator of the observable $\bar{A}$. This is equivalent to the mole fraction of the molecules possessing the measurable quantity. Such an identification is in accordance with the concept of Van Hoff that a filter or a semi-impermeable membrane can be constructed to separate the molecules possessing the quantity ϵ_i from the rest of the ensemble. In quantum mechanics, since not all observables can be measured simultaneously, a different mixing entropy can be associated with each observable. A special role is played by the energy observable. In nondissipative evolution the entropy associated with the energy is conserved. For the entropy associated with other observables Eq. (6.1) in general is not conserved and may even oscillate.

von Neumann introduced the concept that a statistical ensemble of molecules defined by the state $\hat{\rho}$ is classified by an observable $\bar{B}$ which has the minimum dispersion while generating a full resolution of the state of the system.[14,25] This observable can be defined as the one which minimizes Eq. (6.1). The operator $\hat{\mathbf{B}}$ associated with this observable $\bar{B}$ also commutes with $\hat{\rho}$, therefore its spectral resolution has the same set of projection operators. This observable is used to define the von Neumann entropy

$$S_{\mathrm{VN}} = -\mathrm{tr}(\hat{\rho} \log \hat{\rho}). \tag{6.2}$$

For a unitary evolution which is generated by the Hamiltonian part of Eq. (2.5) the von Neumann entropy is a constant of motion as are all traces of analytic functions of $\hat{\rho}$.[26] In thermal equilibrium the von Neuman entropy is identical to the energy entropy $S(\bar{E})=S_{\mathrm{VN}}$ since the density operator commutes with the Hamiltonian.

The entropy analysis of the process is related to the observable by which the analysis is carried out.[25,27] In the radiative system under study an additional restriction of separability is imposed on the observables. These observables are associated with the separation to ground and excited subsystems. For a restricted observable the corresponding operator has the form

$$\hat{\mathbf{O}} = \hat{\mathbf{A}}_{\mathbf{g}} \otimes \hat{\mathbf{P}}_{\mathbf{g}} + \hat{\mathbf{B}}_{\mathbf{e}} \otimes \hat{\mathbf{P}}_{\mathbf{e}} \tag{6.3}$$

with the entropy

$$S(\bar{O}) = xS(\bar{A}_g) + (1-x)S(\bar{B}_e) + S_{\mathrm{mix}}, \tag{6.4}$$

where $S_{\mathrm{mix}} = -x \log x - (1-x)\log(1-x)$ and $x=\langle \hat{\mathbf{P}}_{\mathbf{g}} \rangle$, is the mole fraction in the ground surface. The individual surface entropy $S(\bar{A}_1)$ is defined by Eq. (6.1). The zero order Hamiltonian observable $\hat{\mathbf{H}}_0$ is just such a separable operator and it is of particular interest. Subject to the constraints of separability, the minimum dispersion operator can be considered which will commute with $\hat{\rho}=\hat{\rho}_{\mathbf{g}} \otimes \hat{\mathbf{P}}_{\mathbf{g}} + \hat{\rho}_{\mathbf{e}} \otimes \hat{\mathbf{P}}_{\mathbf{e}}$. This partition means that in each surface the minimum dispersion entropy is found separately leading to

$$S_{R-\mathrm{VN}} = xS_{g-\mathrm{VN}} + (1-x)S_{e-\mathrm{VN}} + S_{\mathrm{mix}}. \tag{6.5}$$

Comparing the different types of entropy, the following inequality is obtained:[28]

$$S_{\mathrm{VN}} \leqslant S_{R-\mathrm{VN}} \leqslant S(\bar{O}), \tag{6.6}$$

where $S_{R-\mathrm{VN}}$ is the restricted minimum dispersion entropy. These entropies are now used to analyze the cooling process. The system to be cooled at $t=0$ is in a thermal state on the ground surface

$$\hat{\rho}_{\mathbf{g}} = \frac{e^{-\beta \hat{\mathbf{H}}_{\mathbf{g}}}}{Z}, \tag{6.7}$$

where $Z = \mathrm{tr}(e^{-\beta \hat{\mathbf{H}}_{\mathbf{g}}})$ is the partition function and β is the reciprocal temperature. Since $\hat{\rho}_{\mathbf{g}}$ in this case commutes with $\hat{\mathbf{H}}_{\mathbf{g}}$ the entropy associated with energy $S(\bar{E})$ is identical to the von Neumann entropy. If a short impulsive pulse is applied, according to the Franck–Condon principle, a portion of the ground surface density is lifted to the excited surface without a change in the state. The entropy analysis at this point is restricted to the choice of observables which can distinguish the two surfaces. For simplicity, an infinitely short first pulse is considered which creates an image of the ground surface state on the excited surface. The restricted minimum dispersion operator will have the entropy

$$S_{R-\mathrm{VN}} = S[\bar{E}_g(t=0)] + S_{\mathrm{mix}}, \tag{6.8}$$

where $1-x$ is the mole fraction transferred to the upper surface by the first pulse. Since the ground and excited state Hamiltonians do not commute, the state created on the excited surface is nonstationary. This means that the entropy associated with the zero order Hamiltonian observable $S(E_0)$ is larger than Eq. (6.8). An examination of the entropy of the ground surface immediately after the first pulse shows that it is identical to the von Neumann entropy. Since the initial state was in thermal equilibrium its entropy is also identical to $S(\bar{E}_g)$. The time derivative of the entropy at $t=0$ can be calculated, since it is in a thermal state, as

$$\frac{dS(\bar{E}_g)}{dt} = \beta \langle \mathscr{L}^*(\hat{\mathbf{H}}_{\mathbf{g}}) \rangle \tag{6.9}$$

and has the same direction as the change in the ground surface energy. In the model calculation, the direction of change in the ground surface energy was chosen to be negative. If the ground surface would stay in a thermal state at all times, this would assure entropy reduction. The change of entropy with time is demonstrated in Fig. 7. The

initial slope corresponds to the rate of Eq. (6.9). As the cooling process proceeds the entropy of the ground state decreases further. Initially after an infinitely impulsive first pulse the ground state energy entropy $S(\bar{E}_g)$ is identical to the minimum dispersion entropy. As the cooling proceeds, however these two entropies depart meaning that the cooling process creates a state which is not stationary under the field free Hamiltonian evolution. The mixing entropy under the condition of zero mass transport is stationary and therefore can be omitted from the analysis. Although Eq. (6.9) cannot assure monotonic decrease of entropy for later times nevertheless the numerical calculation shows that these conditions still apply.

Since the system is not in equilibrium, the definition of temperature is ambiguous. A dynamical reciprocal temperature $\beta(t)$ of the cooling ensemble can be defined by the relation

$$\beta(t)=\frac{dS(\bar{E}_g)}{d\bar{E}_g}=\frac{dS(\bar{E}_g)/dt}{d\bar{E}_g/dt}. \tag{6.10}$$

For a thermal ensemble this reproduces Eq. (6.9). Since the cooling process can be pulsed, numerical evaluation of Eq. (6.10) is troublesome whenever $d\bar{E}_g/dt$ goes to zero. The dynamical temperature can be compared to the temperature of a thermal ensemble which shares the same average energy $\bar{E}_g$. This comparison is shown in Fig. 18. Since large differences are found between the two definitions of temperature it seems that entropy is a superior tool for analysis of the cooling process.

VII. THE THIRD LAW

The choice of phase in Eq. (4.9) leads to a monotonic decrease in the ground surface energy. This decrease is accompanied by a decrease in entropy and temperature. As the ground surface system approaches the absolute zero, it should obey the third law of thermodynamics so that the rate of cooling will also decrease to zero. Using a zero temperature representation of the state on the ground surface $\hat{\rho}_g=|\psi_g(E_0)\rangle\langle\psi_g(E_0)|$, where $\psi_g(E_0)$ is the ground surface zero eigenfunction and $E_g(0)$ is the zero eigenfunction energy. The correlation term of the state $\hat{\rho}$ becomes then

$$\hat{\rho}_i^{\dagger}=\psi_g(E_0)\sum_j c_j\phi_{e_j}^*, \tag{7.1}$$

where ϕ_{ej} is a complete set of excited surface eigenfunctions. For this state

$$\frac{d\langle E_g\rangle}{dt}=C(t)\frac{2}{\hbar}\,\mathrm{Imag}[\Phi(\langle\hat{\mu}\otimes\hat{\mathbf{S}}_-\rangle)\langle\hat{\mu}\otimes\hat{\mathbf{S}}_+\rangle E_g(0)]$$
$$=0 \tag{7.2}$$

which proves that the cooling strategy obeys the third law of thermodynamics. Equation (7.2) can be understood by the observation that once the ground state is approached the flow of mass and energy from this state is stopped effectively isolating this state. Morever this result is also true for any ground surface state that is an eigenvalue of the ground surface Hamiltonian $\hat{\mathbf{H}}_g$, and it becomes a generalization of the third law which states that any approach to an energy eigenstate by a thermodynamic process becomes infinitely slow.

VIII. COOLING SCENARIO AND COMPUTATIONAL DETAILS

The scenario presented in this section has many possibilities. The purpose is to demonstrate a cooling strategy for a particular molecule in different environments, such as collision free conditions or dissipative conditions. In particular the realization the thermodynamic currents presented in Fig. 2 is attempted. The ground and excited surfaces of HBr have been chosen for the demonstration. The potential energy surfaces are shown in Fig. 1. The choice of molecules with a mass which is not heavy is to facilitate the computation effort. Heavier molecules such as I_2 have been tried out and qualitatively it has been found that they are cooled in a similar way.

The computation procedure can be divided into three steps: (1) calculation of the initial thermal state on the ground surface, (2) application of a short impulsive pulse which transfers a small fraction of the population to the excited surface, (3) simulation of the cooling procedure. The first step of calculating the thermal state is done by assemblying it from the set of low lying eigenfunctions of the ground surface Hamiltonian $\hat{\mathbf{H}}_g$. These are calculated on a grid by the relaxation method.[29] From these eigenfunctions projection operators are created which are combined with Boltzmann weights to produce a thermal density operator (6.7). The initial density operator $\hat{\rho}_g$ is shown as a Wigner phase space distribution[30] in Fig. 13. An initial temperature of 5000 K on the ground surface state was chosen.

The second and third steps require the numerical solution of the Liouville von Neumann equation. The method of solution of the Liouville equation is based on that of previous work.[31,32] The density operator as well as other operators are sampled on an evenly spaced grid with an underlying Fourier basis of plane waves. The basic operation of the Liouville operator is the commutation relation. The commutation relation of the state $\hat{\rho}$, in Eq. (2.1) with $\hat{\mathbf{H}}_0$, described in Eq. (2.3), becomes

$$[\hat{\mathbf{H}}_0,\hat{\rho}]=[\hat{\mathbf{H}}_g,\hat{\rho}_g]\otimes\hat{\mathbf{P}}_g+[\hat{\mathbf{H}}_e,\hat{\rho}_e]\otimes\hat{\mathbf{P}}_e$$
$$+(\hat{\mathbf{H}}_e\hat{\rho}_i-\hat{\rho}_i\hat{\mathbf{H}}_g)\otimes\hat{\mathbf{S}}_+ +(\hat{\mathbf{H}}_g\hat{\rho}_i^{\dagger}-\hat{\rho}_i^{\dagger}\hat{\mathbf{H}}_e)\otimes\hat{\mathbf{S}}_-. \tag{8.1}$$

The numerical procedure calculates these commutation relations locally. Each surface Hamiltonian is divided into a kinetic and a potential term: $\hat{\mathbf{H}}_l=\hat{\mathbf{K}}_l+\hat{\mathbf{V}}_l$ ($l\in g,e$). Since the commutation relation is linear, each term is calculated separately and locally. For the commutation relation of the potential with the diagonal blocks of $\hat{\rho}_l$, one obtains

$$([\hat{\mathbf{V}}_l,\hat{\rho}_l])_{ij}=(V_l)_i(\rho_l)_{ij}-(\rho_l)_{ij}(V_l)_j$$
$$=[(V_l)_i-(V_l)_j](\rho_l)_{ij}. \tag{8.2}$$

For the off-diagonal blocks $\hat{\rho}_i\otimes\hat{\mathbf{S}}_+$, a typical term of the commutation relation becomes

TABLE I. Parameters of propagation in a.u.

	$V(r) = D[e^{-2\beta(r-r_{eq})} - 2e^{-\beta(r-r_{eq})}] + V_0$			
Potential	D	β	r_{eq}	V_0
Ground surface	0.177	0.865	2.67	0
Excited surface	0.123	0.98	2.93	0.322
Dipole function	$\mu=ar$	$a=1.0$		
Propagation				
Grid	$\Delta x=7.210^{-2}$	$N_x=64$	$X_{min}=1.78$	
mass	$m=0.996$			
without dissipation	$\Delta t=0.1$	$N_t=33\,000$	Order=3	
with dissipation	$\Delta t=0.02$	$N_t=100\,000$	Order=16	
First pulse	$\epsilon(t)=A(t)\cos(\omega t)$	$A(t) = \alpha e^{-t^2/2\tau^2}$		
	$\omega=0.3217$	$\alpha=0.028$	$\tau=130$	
Cooling pulse	$W=\frac{1}{2}$			
Tolerance	10^{-5}			
Dissipation	$\gamma=0.9$			

$$([\hat{\mathbf{V}},\hat{\rho}_i])_{ij}=[(\mathbf{V}_e)_i-(\mathbf{V}_g)_j](\hat{\rho}_i)_{ij}. \tag{8.3}$$

A similar expression is used for $\hat{\rho}_i^\dagger \otimes \hat{\mathbf{S}}_-$. The operation of the kinetic energy commutation is the same for all blocks of $\hat{\rho}$

$$([\tilde{\mathbf{K}},\tilde{\rho}])_{ij}=(\tilde{\mathbf{K}}\tilde{\rho}-\tilde{\rho}\tilde{\mathbf{K}})_{ij}=\frac{1}{2m}(k_i^2-k_j^2)\tilde{\rho}_{ij}, \tag{8.4}$$

where $\tilde{\mathbf{O}}$ designates the Fourier transformed operator (coordinate to momentum), which is also the momentum representation of the operator. For the interaction part of the Hamiltonian $\hat{\mathbf{V}}_t$ presented in Eq. (2.4) the commutation relation with $\hat{\rho}$ becomes

$$[\hat{\mathbf{V}}_t,\hat{\rho}]=\epsilon(\hat{\rho}_e\hat{\mu}-\hat{\mu}\hat{\rho}_g)\otimes\hat{\mathbf{S}}_+ +\epsilon^*(\hat{\rho}_g\hat{\mu}-\hat{\mu}\hat{\rho}_e)\otimes\hat{\mathbf{S}}_- +\epsilon(\hat{\rho}_i^\dagger\hat{\mu}\otimes\hat{\mathbf{P}}_g-\hat{\mu}\hat{\rho}_i^\dagger\otimes\hat{\mathbf{P}}_e)+\epsilon^*(\hat{\rho}_i\hat{\mu}\otimes\hat{\mathbf{P}}_e-\hat{\mu}\hat{\rho}_i\otimes\hat{\mathbf{P}}_g). \tag{8.5}$$

For the following calculations, a linear dipole function was used. For the calculation which includes dissipation, a pure dephasing Liouville superoperator was introduced

$$\mathscr{L}_D(\hat{\rho})=\gamma[\hat{\mathbf{H}}_g,[\hat{\mathbf{H}}_g,\hat{\rho}]], \tag{8.6}$$

where the parmeter γ is adjusted. The formalism allows more elaborate dissipative terms than Eq. (8.6) but for the purpose of studying the influence of dissipation this term which does not change the ground state energy emphasizes the role of pure dephasing on the cooling process. By summing up these basic operations the evaluation of the Liouville operator $\mathscr{L}(\rho)$ is obtained.

The time propagation is done in small segments Δt in order to overcome the problem of the time dependence of Liouville operator through $\epsilon(t)$. The propagator in each segment is expanded by an interpolation polynomial in the Newton form

$$e^{\mathscr{L}\Delta t}=d_0\mathscr{I}+d_1(\mathscr{L}-x_1\mathscr{I}) +d_2(\mathscr{L}-x_2\mathscr{I})(\mathscr{L}-x_1\mathscr{I})+\cdots, \tag{8.7}$$

where x_i are sampling points and d_i are the divided difference coefficients[32] which are determined by the value of the function $e^{z\Delta t}$ at the sampling points. These sampling points x_i have to span the spectral range of the Liouville superoperator. For nondissipative propagation the sampling points were either the zeros of the Chebychev polynomials adjusted to the estimated spectral range of $\mathscr{L}$ or were calculated by a short iterative Lanczos (SIL) procedure. This procedure becomes a Liouville space generalization of the procedure developed for wave functions.[33,34] For dissipative propagation since the spectral range of $\mathscr{L}$ is complex, the sampling points were chosen evenly spaced on a semicircle in the negative side of the complex plane.[32] Equation (8.7) is then applied recursively on to the density operator $\hat{\rho}(t)$ to obtain $\hat{\rho}(t+\Delta t)$. Table I summarizes the parameters used in the calculation.

The second step in the calculation is to apply a short impulsive pulse in order to transfer a small amount of population from the ground to the excited potential. A pulse duration of 3 fs was used and the amount of population transfer was 11%. This pulse is impulsive on the time scale of vibrational motion of HBr but is not impulsive on the time scale of electronic motion. As a result not all parts of the ground surface density are in resonance with the electronic transition and this causes heating of the ground surface state from 5000 to 6400 K. The preheating effect can be seen by comparing the initial thermal state, displayed in Fig. 13 to the state after the first pulse displayed in Fig. 14. It is apparent from the figures that the latter is much broader. This excitation mechanism has been analyzed previously[35] and verified experimentally.[36,37] A shorter initial pulse will reduce this effect.

The first pulse also establishes a nonzero instantaneous transition dipole expectation value which is the starting point for the cooling pulses. This pulse also synchronizes the molecular motion with the radiation field.

Once a transition dipole has been induced, the cooling cycle of the ground surface can begin. The calculation of the field ϵ for the cooling process by Eq. (5.1) and Eq. (5.5) requires the calculation of the expectation values $\langle\hat{\mu}\otimes\hat{\mathbf{S}}_-\rangle$ and $\langle\hat{\mu}\hat{\mathbf{H}}_g\otimes\hat{\mathbf{S}}_+\rangle$. As these terms in turn also depend on ϵ, a predictor corrector procedure is used where

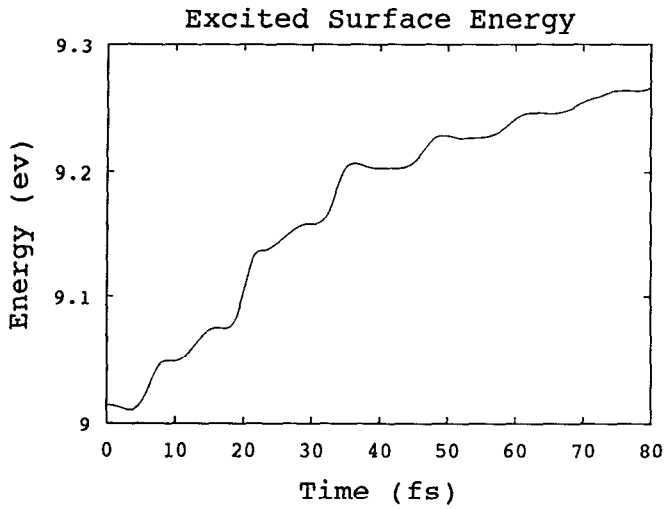

FIG. 5. Excited surface energy $\bar{E}_e$ as a function of time.

the state is propagated for a time step Δt calculating the field ϵ by using the expectation values at the beginning of the time step. The expectation values at the end of the step are calculated and averaged with the ones at the beginning of the step. A new field ϵ is then calculated and used to repropagate $\hat{\rho}$ another time step. This procedure is equivalent to a first order Magnus approximation.[38] Since the propagation includes a feedback term it is sensitive to small numerical errors and therefore presents a major challenge to the numerical procedure. As a result the calculation was executed using double precision arithmetic and very small time steps. The condition of zero mass transport was used to check the accuracy. The ground surface norm was kept constant typically to within 10^{-5}.

The calculation of the state $\hat{\rho}(t)$ as a function of time enables the study of the evolution of relevant expectation values. Figure 4 shows the energy on the ground surface as a function of time demonstrating the monotonic decrease, under the conditions of norm conservation. Figure 5 shows the accompanying increase in the excited surface energy and Fig. 6 is the energy stored in the interaction. The

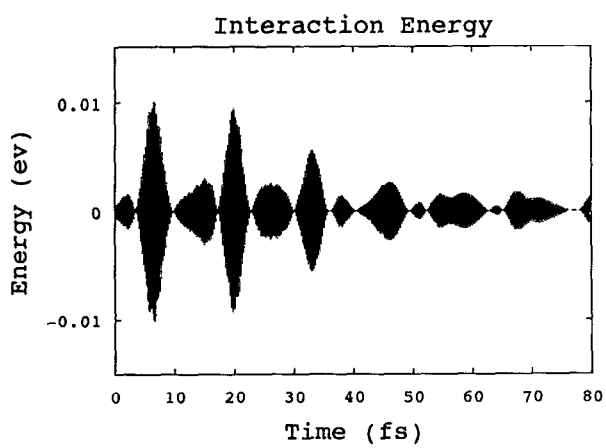

FIG. 6. The interaction energy $\langle \hat{V}_t \rangle$ as a function of time.

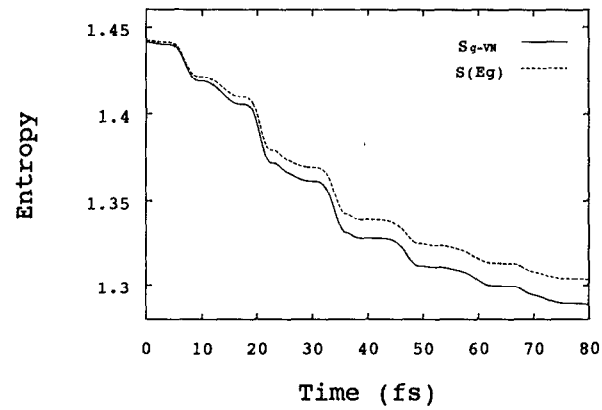

FIG. 7. Ground surface energy entropy $S(\bar{E}_g)$ (solid) and ground surface portion of the restricted von Neuman entropy $S_{g-\mathrm{VN}}$ (dashed) as a function of time for the pulse of Fig. 9.

decrease in the energy in the ground surface is more than compensated by the increase in the energy in the excited surface. This figure emphasizes the heat pump character of the cooling process. The cyclic action of the pump can be seen in Fig. 5 by the fact the interaction energy goes to zero periodically.

The cooling action is shown in Fig. 7 which displays the entropy on the ground surface as a function of time. Both the energy entropy, and the von Neuman entropy on the ground surface decrease monotonically where the energy entropy $S(\bar{E}_g)$ is larger than $S_{g-\mathrm{VN}}$ in accordance with Eq. (6.6). The entropy on the excited surface is shown in Fig. 8. It increases as it should to compensate the decrease in entropy on the ground surface. One should also notice the oscillations in the energy entropy $S(\bar{E}_e)$ due to the fact that the excited surface Hamiltonian is no longer stationary. The decrease in dispersion in the cooling process can also be observed by comparing the state after the first pulse, Fig. 14, to the final state Fig. 15, which is less dispersed in phase space.

The radiative field of the cooling pulse sequence is shown in Figs. 9, 10, and 11. Figure 9 shows the radiation

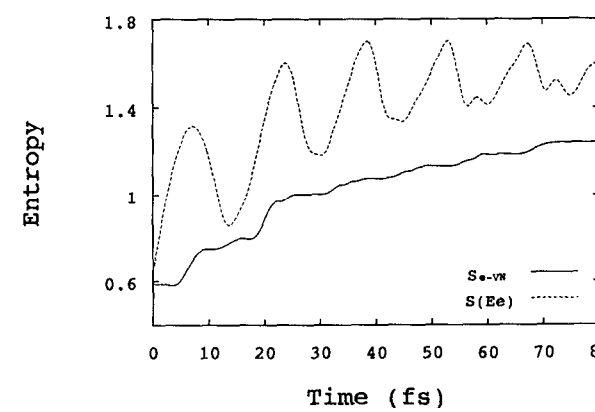

FIG. 8. Excited surface energy entropy (solid) and excited state portion of the restricted von Neuman entropy $S_{e-\mathrm{VN}}$ (dashed) as a function of time for the pulse of Fig. 9.

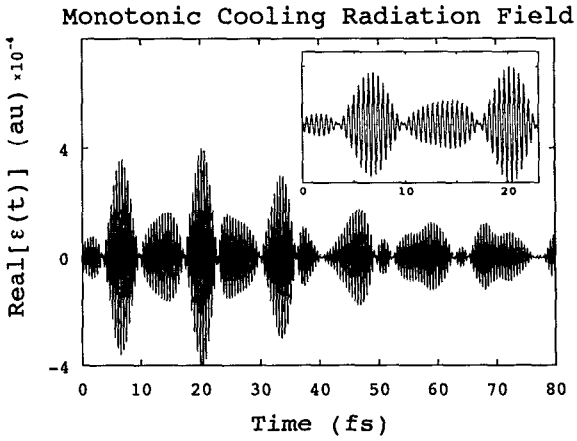

FIG. 9. Real part of the pulse as a function of time for the monotonic decrease in the ground surface energy.

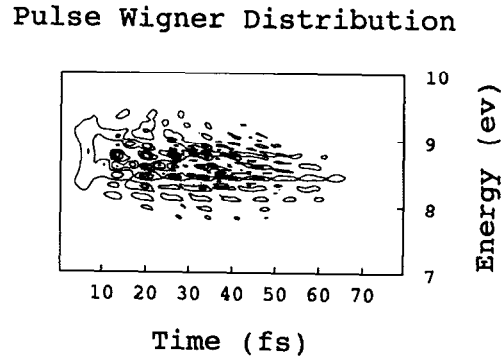

FIG. 11. Wigner distribution function of the pulse of Fig. 9 displayed as a contour plot in the time energy phase space.

field leading to cooling in the time domain. One should notice that the field can be decomposed to a series of pulses with a well defined phase relation. Figure 10 shows the radiation field in the frequency domain. Figure 11 displays the field in the time energy phase space as a Wigner distribution function.[30] From Fig. 11 it is apparent that the pulse looses intensity as time progresses. Since the pulse is determined by the instantaneous dipole this fact reflects the loss of overlap between the ground and excited energy surfaces reducing the ability to cool as time progresses. The decomposition of the field into individual pulses is due to the oscillation of the instantaneous dipole driven by the ground surface and excited surface vibrational motion. This effect can also be seen in the spectrum of the pulse, Fig. 10 which is centered around the electronic transition but is modulated by the vibrational frequencies. The Wigner distribution shows that the pulse becomes weaker as time proceeds reflecting a decrease in the instantaneous dipole.

The next step is to study the influence of dissipation on the energy reduction process. Figure 12 compares the

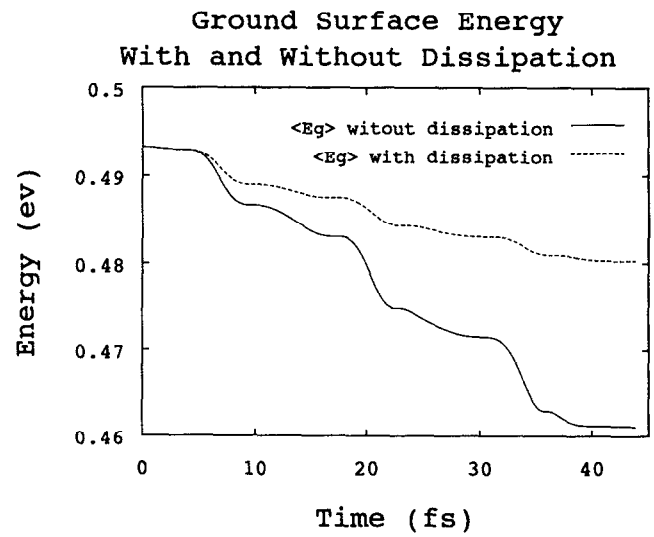

FIG. 12. Comparison of the ground surface energy as a function of time with dissipation (dashed) and without dissipation (solid).

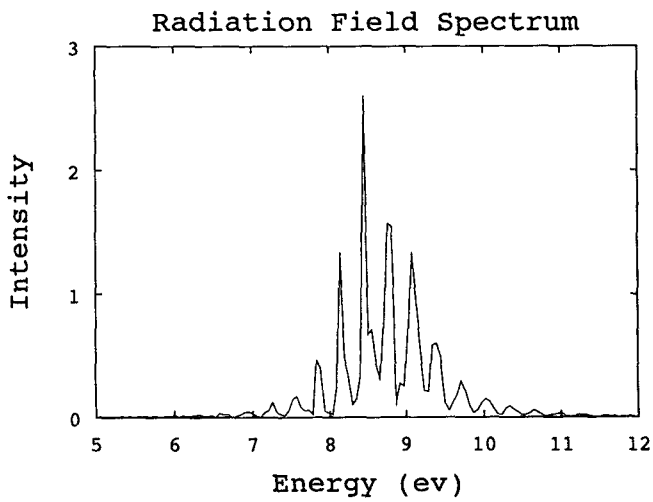

FIG. 10. Spectrum of the pulse of Fig. 9 (arbitrary units).

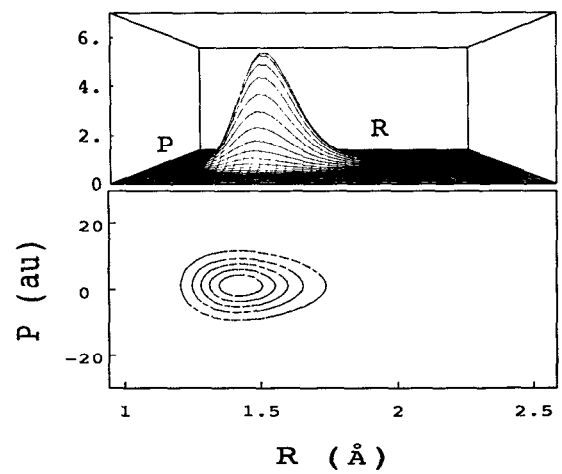

FIG. 13. Phase space display of the initial density operator $\hat{\rho}_g(0)$ (Wigner distribution function in the position momentum phase space). Upper panel stereoscopic projection lower panel contour map.

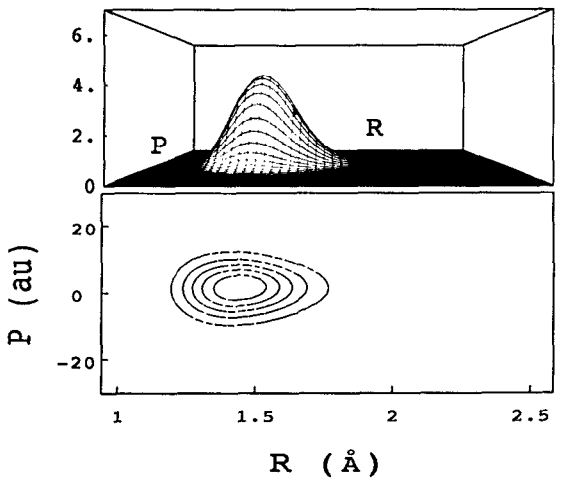

FIG. 14. Phase space display of the density operator after the first excitation pulse. Upper panel stereoscopic projection lower panel contour map.

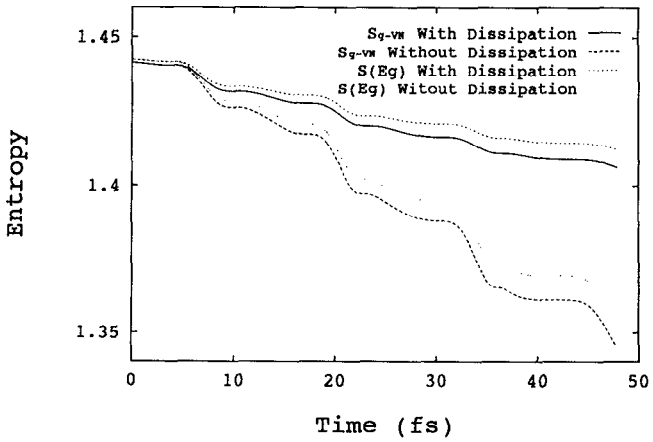

FIG. 16. Comparison between the different entropies: $S(\bar{E}_g)$ and $S_{g-\mathrm{VN}}$ for the ground surfaces as a function of time (with and without dissipation).

ground surface energy for a cooling process with and without dissipation. It is apparent that the dissipation reduces the rate of cooling. (See Figs. 13–15.) Figure 16 is a comparison of the entropy reduction during cooling with and without dissipation on the ground surface while Fig. 17 compares the entropies on the excited surface. The dissipation reduces both the entropy decrease on the ground surface as well as the increase on the excited surface. In general, it can be said that dissipation is harmful to the cooling process. Although the particular dissipation superoperator, $\mathcal{L}_D$ in Eq. (8.6), can only cause loss of phase and cannot influence directly the ground surface energy.

Figure 18 shows the temperature of the ground surface ensemble as a function of time. The temperature calculated according to Eq. (6.10) is compared to the temperature of a thermal ensemble with the same average energy. The numerical difficulties which occur when the cooling rate goes to zero are clearly seen. Figure 19 shows that the relation between the ground surface energy and the entropy is well behaved which emphasizes that entropy is a better variable than temperature in analyzing the cooling action.

IX. DISCUSSION

The numerical model presented in Sec. VIII is sufficient to show that a thermodynamic analysis and the phase control mechanism can be used to promote cooling in a realistic molecule. Nevertheless, it is premature to apply directly the demonstrated scenario since it is far from optimal. Experimental verification therefore, will require further study of optimization schemes. For example, a cooling strategy based on maximizing the time derivative of the energy difference $d/dt(E_e-E_g)$ has been found to be superior to the strategy based on maximizing the energy flow $-(dE_j/dt)$. A comparison of the energy reduction of these two strategies is shown in Fig. 20. Another possibility is to tune the radiation to maximize the entropy flow

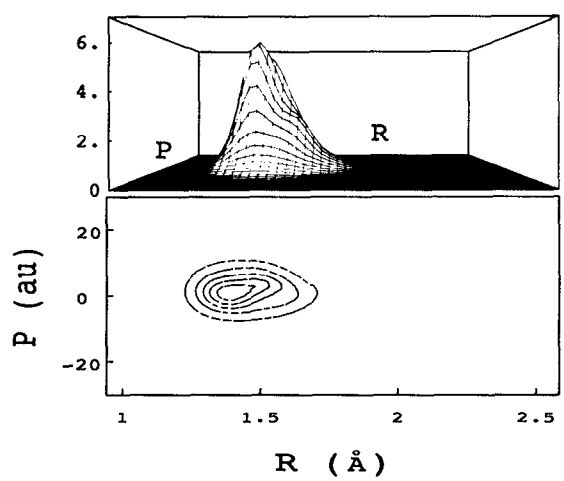

FIG. 15. Phase space display of the final density operator without dissipation $\hat{\rho}_g(t_f)$. Upper panel stereoscopic projection lower panel contour map.

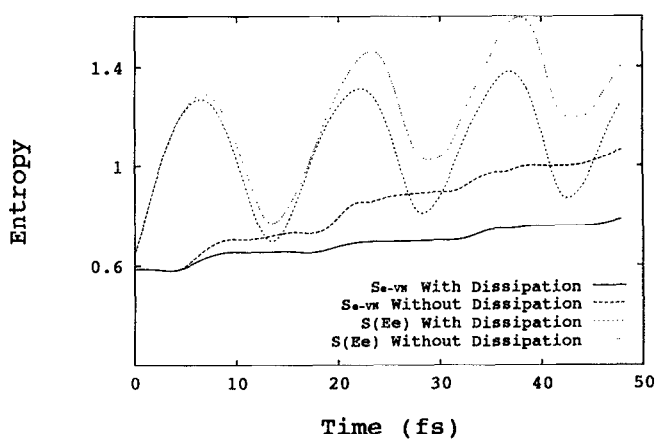

FIG. 17. Comparison between the different entropies: $S(\bar{E}_e)$ and $S_{e-\mathrm{VN}}$ for the excited surfaces as a function of time (with and without dissipation).

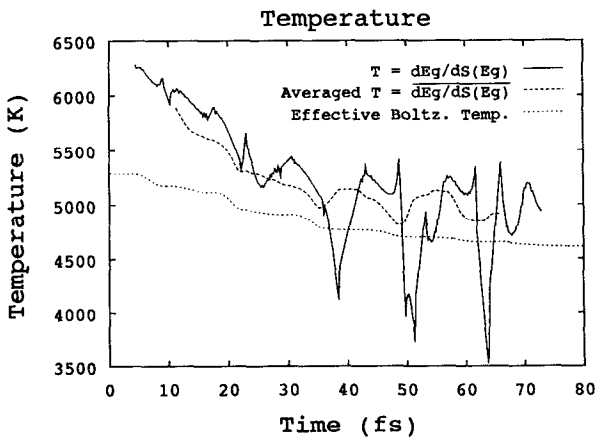

FIG. 18. Temperature and averaged temperature as a function of time compared to an effective temperature of an ensemble with the same energy.

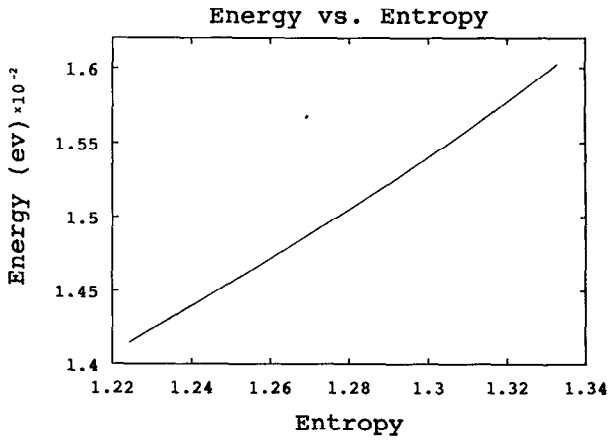

FIG. 20. Comparison of different cooling strategies: ground surface energy as a function of time. The same initial pulse was used for the two cases.

$-(d/dt)S_g$ which is a strategy to reduce the dispersion directly. An important issue is the optimization of the first synchronizing pulse. A short pulse which has a frequency bandwidth larger than the thermal absorption spectra causes no preheating of the molecular ensemble. This is in contrast to the 3 fs pulse used in the demonstration which caused significant preheating. This heating effect could have been reduced by detuning the pulse frequency below the vertical transition frequency leading to some initial evaporative cooling.[39] Finally an effective optimal cooling strategy should merge the role of the synchronization pulse and the cooling pulse leading to a combination of an evaporative and pumping cooling mechanisms. This strategy relaxes the strict zero mass transport condition replacing it with an asymptotic restriction on the total amount of population left on the ground surface. An ultimate global optimal cooling strategy is beyond the scope of this paper aimed at gaining insight into thermodynamical analogies based on a local-in-time approach.

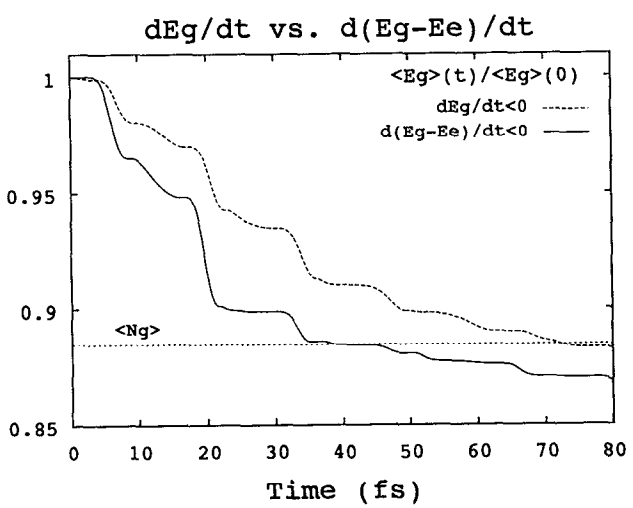

FIG. 19. Ground surface energy as a function of entropy.

Another angle on the optimization problem can be obtained by employing the field of finite time thermodynamics. This discipline studies the performance of thermodynamic processes restricted to taking place in a finite time. The analysis goes beyond the traditional adiabatic thermodynamic description.[40] Most of the work in finite time thermodynamics has been devoted to the optimization of heat engines,[41] including quantum mechanical models of such engines.[19,20,42] The generic picture that emerges from these studies is that the power output of the engines goes through a maximum as a result of a balance between maximizing the flow and minimizing the loss mechanisms. As a result, at maximum power operation conditions, engine efficiency is reduced from the Carnot adiabatic value. Applications of finite time thermodynamics to cooling are limited[43] none of which include a quantum mechanical analysis. These analogies with finite time thermodynamics require further persuit since the impulsive nature of the process leads to the breakdown of the adiabatic theorem which is also the source of irreversibility in finite time thermodynamics.[20]

One of the difficulties of the thermodynamical analysis stems from the fact that entropy and temperature seem to be ambiguous. Even the energy is an ambiguous quantum mechanically for a nonstationary state. For that matter, there is a problem in classical thermodynamics defining temperature and entropy if equilibrium conditions do not apply. For example, at equilibrium one can define temperature as that quantity which becomes equal for bodies in thermal contact. Here there is no analog of heat transfer. There is another quantum source of irreversibility which stems from the local partition to the ground and excited surfaces. This partition restricts the class of observables which can be used to analyze the state leading to the loss of information in the nondiagonal blocks of the density operator. An analysis by Lindblad[44] of the quantum mechanical measurement process has identified a similar source of irreversibility due to the partition of the system into a measured part and a measuring apparatus.

Experimental realization of laser cooling is closely linked to the technology of ultrafast pulse shaping. This technology is undergoing rapid development where the light pulses have become shorter and more powerful. Pulse shaping techniques able to control the amplitude and phase of the pulse are becoming available.[8,45–47] Specifically the experimental setup used by Sherer *et al.*,[8] for the I_2 system, is closely related to the control conditions on the phase angle of Sec. IV. In this experiment the flow of population from the ground X state to the excited B state was controlled by manipulating the time delay and the relative phase between two pulses experimentally confirming Eq. (4.6). A small modification of this experiment which amounts to shifting the relative phase angle by $\pm\pi/2$, could, in principle, lead to zero mass transport conditions of Eq. (4.9) which is the prerequisite for cooling conditions. The experimental progress leads to an optimistic forecast for future heat pump cooling of molecular matter.

At this point, a comparison of laser translational cooling with laser internal cooling is in place. As was stated in the introduction, translational cooling is driven by the entropy increase of the radiation which initially was a coherent geometrically well-defined beam of light. Due to its interaction with the atoms it scattered into a nonisotropic state with increased entropy. For this reason this process can be defined as evaporative. In this study the radiation is used as pure work under the assumption that on the time scale of the cooling process spontaneous emission with entropy increase can be neglected. Also in the heat pump the cooling mechanism requires synchronization between the radiation and the molecular motion. Another distinction between the two processes is that in the translational cooling the frictional force is external and acts on the spatial coordinate of the atom confining it in space. On the other hand, the force in Eq. (3.11) operates on internal degrees of freedom. Finally, an important similarity exists between the translational evaporative cooling and the heat transfer cooling in that the radiation is manipulated in such a way that when the system approaches the target state it stops to absorb the light. As analyzed in Ref. 48 and shown in Eq. (7.2) the state becomes stationary. These conditions are responsible for the compliance with the third law of thermodynamics.

The analysis of the control of transport in Sec. IV shows that a crucial condition for control is the maintenance of well defined phase relation between the ground and excited surfaces. This phase relation appears as a nonvanishing instantaneous dipole expectation $\langle\hat{\mu}\otimes\hat{S}_+\rangle$. Any degradation of this phase relation will reduce the control options. One reason for loss of control is anharmonic motion which can cause dephasing of a compact excited state. In the HBr molecule this effect has been found to be nonsignificant. Another dephasing mechanism is the result of strong radation fields.[49] It was found that strong radiation tends to scatter the excited surface state. The third and most important dephasing mechanism is the result of dissipation. Equation (5.9) demonstrates how the control possibilities are influenced by the backward propagation of the target function. If this backward propagation is dissipative the ability to control the process is degraded. Specifically, the dissipative mechanism used in the calculation commutes with the target function. This means that the loss of control is a second order process, but nevertheless, the calculation shows significant loss of control. Quantitatively the dephasing that was used in the calculation is quite strong. This means that even under strong collision environment cooling is possible. The relative importance of different dissipative mechanisms such as direct energy relaxation and electronic relaxation is under study.

X. SUMMARY

(1) The interaction of light with a two electronic surface system, bears close analogies to the thermodynamics of two coupled systems which can transfer mass and energy via external work Fig. 2. A version of the first, second, and third law of thermodynamics was presented. Moreover, various processes which transfer energy without mass and mass without energy were identified.

(2) The paper focuses then on a particular process: transferring energy without mass to the excited electronic surface. This is laser cooling. First, a local in time procedure to find the field to accomplish this was given; then an optimal control formulation was sketched.

(3) Numerical results were presented for laser cooling by solving the quantum Liouville equation, with and without dissipation. Starting with a Boltzmann distribution characterized by temperature T, the cooling field reduced the dispersion, narrowing the phase space distribution. Vibrational dephasing reduced the ability to cool the system by the heat pump mechanism.

Finally, this paper is on one hand a continuation of effort devoted to laser selective chemistry but on the other hand, it opens a new field of radiative cooling and as such raises more questions than answers.

ACKNOWLEDGMENTS

We wish to thank Stuart Rice for his help and many stimulating discussions. The help of Audrey Del Hammerich and Eitan Geva is also appreciated. This research was supported by the Binational United States–Israel Science Foundation and the Office of Naval Research. The Fritz Haber Research Center is supported by the Minerva Gesellschaft für die Forschung, GmbH München, FRG.

[1] D. H. Levy, Annu. Rev. Phys. Chem. **31**, 197 (1980).
[2] C. N. Cohen-Tannoudji and W. D. Phillips, Phys. Today **43**, 33 (1990).
[3] S. Chu, Science, **253**, 861 (1991).
[4] S. Rice, Science **258**, 412 (1992).
[5] G. W. Coulston and K. Bergmann, J. Chem. Phys. **96**, 3467 (1992).
[6] M. Shapiro and P. Brumer, J. Chem. Phys. **84**, 4103 (1986); Acc. Chem. Res. **22**, 407 (1989).
[7] R. Kosloff, S. A. Rice, P. Gaspard, S. Tersigni, and D. J. Tannor, Chem. Phys. **139**, 201 (1989).
[8] N. F. Scherer, R. J. Carlson, A. Matro, M. Du, A. J. Ruggiero, V. Romero-Rochin, J. A. China, G. R. Fleming, and S. A. Rice, J. Chem. Phys. **95**, 1487 (1991).
[9] D. Tannor and S. A. Rice, J. Chem. Phys. **83**, 5013 (1985); D. Tannor, R. Kosloff and S. A. Rice, *ibid.* **85**, 5805 (1986).
[10] S. Shi, A. Woody, and H. Rabitz, J. Chem. Phys. **88**, 6870 (1988); S. She and H. Rabitz, Comp. Phys. Commun. **63**, 71 (1991).

[11] P. Gross, D. Neuhauser, and H. Rabitz, J. Chem. Phys. **96**, 2834 (1992).
[12] R. Kosloff, A. Hammerich, and D. Tannor, Phys. Rev. Lett. **69**, 2172 (1992).
[13] K. Nelson, in *Mode Selective Chemistry, Jerusalem Symposium on Quantum Chemistry and Biochemistry*, edited by J. Jortner (Kluwer Academic, Dordrecht, 1991), Vol. 24, p. 527.
[14] J. von Neumann, *Mathematical Foundations of Quantum Mechanics* (Princeton University, Princeton, 1955).
[15] G. Lindblad, Commun. Math. Phys. **48**, 119 (1976).
[16] V. Gorini, A. Kossakowski, and E. C. G. Sudarshan, J. Math. Phys. **17**, 821 (1976).
[17] R. Alicki and K. Landi, *Quantum Dynamical Semigroups and Applications* (Springer, Berlin, 1987).
[18] E. B. Davis, *Quantum Theory of Open Systems* (Academic, London, 1976).
[19] R. Kosloff, J. Chem. Phys. **80**, 1625 (1984).
[20] E. Geva and R. Kosloff, J. Chem. Phys. **97**, 4398 (1992).
[21] T. Seideman and M. Shapiro, J. Chem. Phys. **88**, 5525 (1988).
[22] Y. Yan, R. E. Gillian, R. W. Whitnell, K. Wilson, and S. Mukamel, J. Phys. Chem. (1993).
[23] D. Tannor and V. Orlov, Proceedings of the Snowbird NATO workshop on "Time dependent quantum mechanical methods" (1992).
[24] A. Einstein, Verh. d. Dtsch. Physik. Ges. **16**, 820 (1914).
[25] R. Kosloff, Adv. Chem. Phys. **46**, 153 (1980).
[26] Y. Allhasid and R. Levine, Phys. Rev. A **18**, 89 (1978).
[27] A. Lande, *New Foundations of Quantum Mechanics* (Cambridge, 1965).
[28] G. Lindblad, Commun. Math. Phys. **28**, 245 (1972).
[29] R. Kosloff and H. Tal-Ezer, Chem. Phys. Lett. **127**, 223 (1986).
[30] E. P. Wigner, Phys. Rev. **40**, 749 (1932); M. Hillery, R. F. O'Connell, M. O. Scully, and E. P. Wigner, Phys. Rep. **106**, 121 (1984).
[31] M. Berman and R. Kosloff, Compu. Phys. Commun. **63**, 1 (1991).
[32] M. Berman, R. Kosloff, and H. Tal-Ezer, J. Phys. A **25**, 1283 (1992).
[33] C. Leforestier, R. Bisseling, C. Cerjan, M. Feit, R. Friesner, A. Guldberg, A. D. Hammerich, G. Julicard, W. Karrlein, H. Dieter Meyer, N. Lipkin, O. Roncero, and R. Kosloff, J. Comp. Phys. **94**, 59 (1991).
[34] H. Tal-Ezer, R. Kosloff, and C. Cerjan, J. Comp. Phys. **100**, 179 (1992).
[35] B. Hartke, R. Kosloff, and S. Ruhman, Chem. Phys. Lett. **158**, 238 (1989).
[36] T. Baumert, U. Engel, C. Meier, and G. Gerber, Chem. Phys. Lett. **200**, 448 (1992).
[37] U. Banin and S. Ruhman, J. Chem. Phys. **98**, 4391 (1993).
[38] W. Magnus, Commun. Pure Appl. Math. **7**, 649 (1957). R. D. Levine, *Quantum Mechanics of Molecular Rate Processes* (Oxford University, Oxford, 1969).
[39] U. Banin, R. Kosloff, A. Bartana, and S. Ruhman (in preparation).
[40] *Finite Time Thermodynamics and Thermoeconomics*, Advances in Thermodynamics, Vol. 4, edited by S. Sieniutycz and P. Salamon (Taylor and Francis, London, 1991).
[41] F. L. Curzon and B. Ahlboron, Am. J. Phys. **43**, 22 (1975).
[42] E. Geva and R. Kosloff, J. Chem. Phys. **96**, 3054 (1992).
[43] J. M. Gordon I. Rubinstein, and Y. Zermi, J. Appl. Phys. **67**, 81 (1990); D. C. Agrawal and V. J. Menon, Eur. J. Phys. **11**, 305 (1990).
[44] G. Lindblad, Commun. Math. Phys. **40**, 147 (1975).
[45] J. Chesnoy and A. Mokhtari, Phys. Rev. A **38**, 3566 (1988).
[46] A. M. Weiner, D. E. Leaird, G. P. Weiderrecht, and K. Nelson, J. Opt. Soc. Am. B **8**, 1264 (1991).
[47] A. M. Weiner, J. P. Heritage, and E. M. Kirshner, J. Opt. Soc. Am. B **5**, 1563 (1988).
[48] A. Aspect, E. Arimondo, D. Kaiser, N. Vansteenkiste, and C. Cohen-Tannoudji, Phys. Rev. Lett. **61**, 826 (1988); A. Aspect, J. Dalibard, H. Heidmann, C. Salomon, and C. Cohen-Tannoudji, Phys. Rev. Lett. **57**, 1688 (1986).
[49] A. D. Hammerich, R. Kosloff, and M. A. Ratner, J. Chem. Phys. **97**, 6410 (1992).